

Max L. Dupilka and Gerhard W. Reuter*

Dept. of Earth and Atmospheric Sciences, University of Alberta, Edmonton, Canada

1. INTRODUCTION

The character of vertical wind shear appears to play a significant role in tornado development. However, it remains uncertain whether tornadic storms develop in shear environment markedly different from non-tornadic severe thunderstorms and whether the intensity of tornadic storms is related to the amount of wind shear. Thompson et al. (2003) categorized three groups of severe storms as non-tornadic, weakly tornadic (F0-F1), and significantly tornadic (F2 and greater). They found the 0-1 km vector shear magnitude showed discrimination between the significant tornadic and non-tornadic events while the 0-6 km vector shear magnitude discriminated between supercells and non-supercells but not between tornadic and non-tornadic events. Rasmussen and Wilhelmson (1983) proposed that non-rotating thunderstorms could be found in environments of low shear and low convective available potential energy (CAPE) while tornadic storms tended to occur with moderate-strong shear ($> 3.5 \times 10^{-3} \text{ s}^{-1}$) and high CAPE ($> 2500 \text{ J kg}^{-1}$). Studies (e.g. Rasmussen and Blanchard 1998) emphasize that severe thunderstorms and tornadoes occur within a broad range of shear and CAPE environments. A useful concept to analyze storm rotation may be storm-relative helicity (SRH; Davies-Jones et al. 1990). However, the magnitude of SRH depends critically on the storm motion.

The strength and persistence of the rear-flank downdraft (RFD) may be critical for the formation of a low-level mesocyclone and possible tornadogenesis. It has been speculated that thermodynamic differences may exist between RFDs associated with tornadoes compared to those associated with non-tornadic supercells (Markowski et al. 2002). They suggested that evaporative cooling and entrainment of mid-level potentially cold air play a smaller role in the formation of RFDs associated with tornadic supercells compared to non-tornadic supercells. The amount of water vapor available to the storm should affect the potential for evaporation and generation of vorticity (Brooks et al. 1994). Greater water vapor in an airmass may mean there could be less evaporative cooling. A parameter suitable to quantify the amount of water vapor potentially available is precipitable water (PW). We

investigated whether environmental sounding parameters, such as bulk shear, buoyant energy, storm-relative helicity and precipitable water can be used to distinguish between tornadic and non-tornadic severe storms in central Alberta.

Composite weather charts, which employ synoptic and meso-scale patterns associated with defined weather events, are routinely used in many weather offices. Chisholm and Renick (1972) constructed wind shear composite hodographs for three types of storms observed during the Alberta Hail studies project: short-lived single cell storms, multicell storms, and long-lived supercell storms. Single cell storms were associated with light winds ($< 10 \text{ m s}^{-1}$) and little or no vertical wind shear. Multicell storms developed in an environment with unidirectional winds and moderate wind shear (0-6 km shear vector magnitude $\sim 20 \text{ m s}^{-1}$). Supercell storms had rapidly veering winds from southeast in the low levels (below $\sim 2 \text{ km}$) to southwest aloft and strong wind shear (0-6 km shear vector magnitude $\sim 35 \text{ m s}^{-1}$). We constructed composite soundings for three storm categories consisting of non-tornadic severe thunderstorms, weak tornadic and significant tornadic storms (defined in section 2).

This paper deals with forecasting the potential for tornadic development, given the existence of a thunderstorm, in the province of Alberta in Canada. During the summer months, severe convective storms with hail and, occasionally, tornadoes are often formed over Alberta, (Fig. 1) Canada. On average, about 10 tornadoes occur over Alberta each year (Hage 2003).

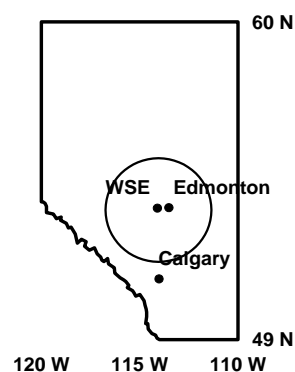


Fig. 1. Outline of Alberta showing the locations of the upper air station at Stony Plain (WSE) and the cities of Edmonton and Calgary. The circle marks the 200 km radius from WSE.

*Corresponding authors address: Dr. Gerhard W. Reuter, Department of Earth and Atmospheric Sciences, University of Alberta, 1-26 Earth Sciences Building, Edmonton, Alberta, T6G2E3, Canada.
E-mail: Gerhard.Reuter@ualberta.ca

2. OBSERVATIONS AND METHODS

Here we present a brief discussion of the methodology used to construct the storm climatology data set. For a detailed discussion the reader is referred to Dupilka and Reuter (2006a). The data set consists of 87 severe storm events occurring within 200 km of Stony Plain, Alberta (WSE; Fig. 1) between 1967 and 2000. All non-tornadic severe storms produced hail with sizes reported as 3 cm or larger. This resulted in 74 tornado and 13 non-tornado severe thunderstorm events. The F0 tornado events dominate (49 cases) out of the total 74 cases. There were 12 F1 tornadoes, 6 F2 tornadoes, and 6 F3 tornadoes. We categorized the tornadic events into two separate classes: significant tornado (ST) events that consisted of F2, F3 and F4 tornadoes, and weak tornado (WT) events that consisted of F0 and F1 tornadoes.

Sounding data were obtained from a CD-ROM, *Rawinsonde Data of North America 1946-1992*, and through an on-line database (post 1992) produced jointly by the National Climate Data Center (NCDC) and the Forecast Systems Laboratory (FSL). Environmental Research Services software package (RAOB) was used to display and analyze sounding data. The RAOB software was used to interpolate the data to 10 mb intervals beginning at 920 mb (approximately the surface pressure in central Alberta). Composite soundings were then constructed for the three groups of storms (NT, WT, and ST) by averaging the temperature, dewpoint, and wind at each pressure level. Wind was partitioned into its zonal and meridional (u , v) components and then each component averaged to construct composite hodographs.

3. RESULTS

3.1. Bulk shear

We computed bulk shear in the layers from 900-800 mb (SHR8), 900-700 mb (SHR7), 900-600 mb (SHR6), and 900-500 mb (SHR5). Figure 2 shows box and whisker plots for bulk shear (SHR8, SHR7, SHR6, and SHR5) values. For the 900-800 mb shear the median for the NT case was $5.0 \text{ m s}^{-1} \text{ km}^{-1}$, for the WT case it was lowest at $4.1 \text{ m s}^{-1} \text{ km}^{-1}$, while the ST case was greatest at $7.4 \text{ m s}^{-1} \text{ km}^{-1}$. For the 900-500 mb shear the median for the NT case was $3.4 \text{ m s}^{-1} \text{ km}^{-1}$, for the WT case it was again lowest at $2.2 \text{ m s}^{-1} \text{ km}^{-1}$, and the ST case was largest at $5.0 \text{ m s}^{-1} \text{ km}^{-1}$. For all four layers shown, the median shear values for ST cases were larger than for WT or NT cases. A similar finding is apparent in the 50% gray boxes. The 50% boxes of shear values for the ST events showed little overlap with the WT cases and generally small overlap with the NT cases. For instance, in the 900-500 mb layer, the 25th percentile for the ST ($4.3 \text{ m s}^{-1} \text{ km}^{-1}$) cases is separated from the 75th percentile for WT cases ($3.8 \text{ m s}^{-1} \text{ km}^{-1}$) and only slightly overlapping the NT 50% box (75th percentile of $4.8 \text{ m s}^{-1} \text{ km}^{-1}$).

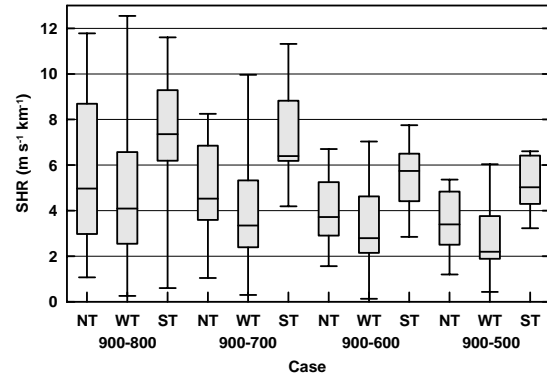


Fig. 2. Box and whisker plots of bulk shear (SHR) values for non-tornado (NT) and tornado (WT, ST) cases in the layers 900-800, 900-700, 900-600, and 900-500 mb. Gray boxes denote 25th to 75th percentiles, with a heavy solid horizontal bar at the median value. The vertical lines (whiskers) extend to the maximum and minimum values. The vertical lines (whiskers) extend to the maximum and minimum values.

For all four layers, the WT 50% boxes were consistently lowest. The NT 50% boxes were slightly higher than the WT cases but, generally with a large overlap between these two events. A Mann-Whitney statistical test (e.g. Miller et al. 1990) for the SHR8 and SHR5 parameters found statistically significant differences at the 1% level between the ST and WT events. Statistically significant differences at the 3-5% level were found for NT-WT pairs based on SHR5, and also NT-ST pairs based on SHR7. There were no significant differences between NT-WT pairs based on SHR8, SHR7 and SHR6 shears. Overall, SHR5 showed statistically significant differences at the 5% or less level between all three categories. This suggests that the bulk shear for the 900 to 500 mb layer provides slightly better assistance in discriminating between ST, WT, and NT cases.

3.2 Convective available potential energy

Most unstable convective available potential energy (MUCAPE) is computed using the virtual temperature of the most unstable parcel in the lowest 300 mb (Doswell and Rasmussen 1994). Figure 3 compares the box and whisker plots for the three storm groups. The ST and NT events had similar median MUCAPE values of about 1050 J kg^{-1} while the WT events had the lowest median value ($\sim 900 \text{ J kg}^{-1}$). There is no trend toward increasing MUCAPE values being associated with NT through ST storms. This suggests that MUCAPE alone offers little help in predicting the likelihood of tornado formation or about the likely intensity of the tornado should it form.

3.3 Storm-relative helicity (SRH)

Values of SRH were calculated for 0-1 km and 0-3 km AGL layers. The storm motion was estimated using Bunkers's method (Bunkers et al. 2000). Figure 4a compares box and whisker plots of the 0-1 km SRH

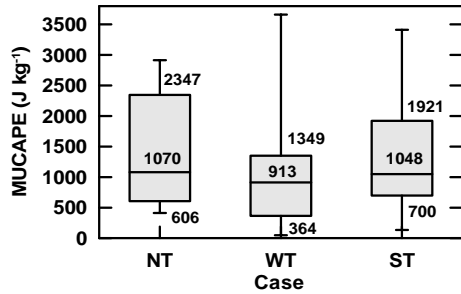


Fig. 3. Box and whiskers plots of MUCAPE for non-tornado (NT) and tornado (WT, ST) cases.

results for the ST, WT and NT storms. There was a slight separation of the SRH values between the three cases, with the 50% boxes showing a general increase from NT to WT to ST events. The median values rose from 7 (NT) to 19 (WT) to 60 $m^2 s^{-2}$ (ST). A Mann-Whitney test showed the only statistically significant difference at the 5% level for SRH values occurred between the WT and ST cases. Values of 0-3 km SRH (Fig. 4b) showed a marked difference between the ST events and the other two cases. The median values were 104 (NT), 71 (WT), and 184 $m^2 s^{-2}$ (ST). Mann-Whitney tests confirmed that 0-3 km SRH values for ST events differ from the other two events at the 1% or less level. There was no statistically significant difference between NT and WT values. The 50% box for ST and WT 0-3 km SRH values ranged from about 140 to 230 $m^2 s^{-2}$ for ST storms, compared to 30-130 $m^2 s^{-2}$ for the WT storms.

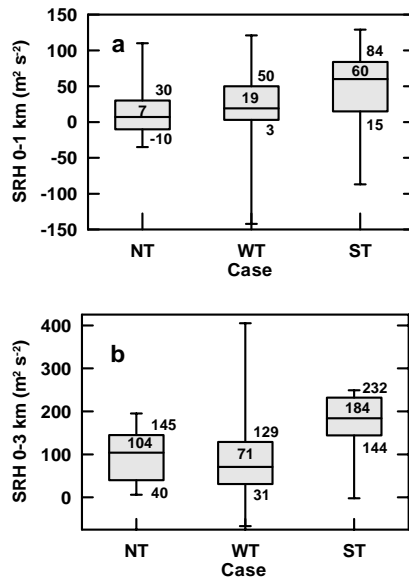


Fig. 4. Box and whiskers plots of SRH estimated via the Bunkers et al. (2000) storm motion algorithm for NT, and WT and ST tornado cases. a) shows SRH in the 0-1 km AGL layer; b) shows SRH in the 0-3 km AGL layer.

3.4 Precipitable water

The values of precipitable water (PW) for each of the cases in our study are shown in Fig. 5. The median values were 23 (NT), 22 (WT) and 25 (ST) mm. For all cases the 50% box of the PW values encompassed a rather limited range from about 20 to 32 mm with the NT and WT events on the lower end of the range (20-25 mm) and the ST events at the upper end (23-32 mm). This might tentatively suggest that, for our sample, there may have been a greater risk for developing severe thunderstorms (which may then spawn tornadoes) when the environment of the developing storm had values of $PW \geq 20$ mm. Precipitable water values above 20 mm are rare in Alberta where average PW for all thunderstorms is about 15 mm. Mann-Whitney test results show the difference in values of PW between ST and the other two cases WT cases are statistically significant at the 5% or less confidence level. Clearly, the amount of PW is only a single integrated value for the amount of water vapor in the atmosphere, while the details the humidity profile likely affect storm evolution. To this end, we examined the tropospheric humidity (TH) values of each event. The TH is defined as the ratio of precipitable water to saturation precipitable water (Bluestein and Jain 1985). The saturation precipitable water depends on the temperature profile, rather than the dewpoint profile used for PW. There was a tendency for PW and TH values to be positively correlated, especially for the ST cases (Dupilka and Reuter 2006b) Higher TH values and, thus, greater PW values might be indicative for weaker evaporative cooling, and a relatively warmer RFD.

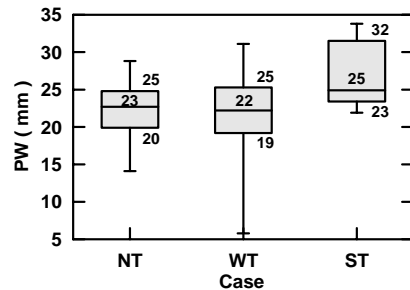


Fig. 5. Box and whiskers plot of Precipitable Water (PW) for non-tornado (NT) and tornado (WT, ST) cases.

4. ASSESSING THE RISK FOR SIGNIFICANT TORNADOES

The Alberta data suggest that SHR8 and SHR5 values provide information concerning the conditional likelihood of tornado formation given the occurrence of a severe storm. The scatter plot of SHR5 and SHR8 values (Fig. 6) suggests that a pair of SHR5 and SHR8 threshold values might be more useful than either shear parameter threshold alone to distinguish between ST and WT cases. Figure 6 shows two specific cases of threshold pairs. Using the threshold pair ($SHR5 = 3 m s^{-1}$

1 km^{-1} , $\text{SHR8} = 6 \text{ m s}^{-1} \text{ km}^{-1}$) 77 % of all ST events occurred within this parameter space whereas only 18 % of the WT events were contained here (solid box in Fig. 6). Also, only 23% of the NT cases occurred here. This suggests that the threshold pair ($\text{SHR5} = 3 \text{ m s}^{-1} \text{ km}^{-1}$, $\text{SHR8} = 6 \text{ m s}^{-1} \text{ km}^{-1}$) offers some skill in providing probabilistic guidance about the conditional likelihood of significant tornadoes versus non-significant tornadoes. Specifically, it was found that only 23% of all ST events had SHR5 and SHR8 values that lay outside of the quadrant ($\text{SHR5} \geq 3 \text{ m s}^{-1} \text{ km}^{-1}$, $\text{SHR8} \geq 6 \text{ m s}^{-1} \text{ km}^{-1}$) Lowering the SHR8 threshold to zero (indicated as the dashed line in Fig. 6) would capture *all historic* ST cases for Alberta.

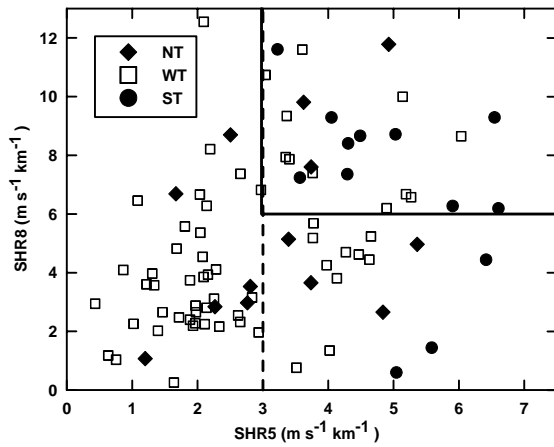


Fig. 6. Scatter plot of SHR8 versus SHR5 for the 87 Alberta storms categorized into NT (diamonds), WT (squares) and ST (dots) cases. The solid (dashed) line marks the 77% (100%) threshold for ST events.

It is similarly instructive to consider the scatter plot of PW versus SHR5 values (Fig. 7). The significant tornado events (dots) occur mostly in the upper right quadrant. For all ST cases, 77% (solid line in Fig. 8) occurred within the quadrant ($\text{SHR5} \geq 3 \text{ m s}^{-1} \text{ km}^{-1}$, $\text{PW} \geq 23 \text{ mm}$). Reducing the moisture threshold to $\text{PW} = 21 \text{ mm}$, would identify all ST cases, but with many WT and NT cases as well (dashed line in Fig. 7).

Depending on the objectives of a probabilistic forecast of ST events, one might select “optimal” threshold pair values for (SHR5 , SHR8) or (SHR5 , PW). If it essential to have a high “Probability of Detection” one should use relatively low values for thresholds. In contrast, if it is essential to have a low “False Alarms Ratio” then this implies higher threshold values.

5. COMPOSITE SOUNDINGS

5.1 Temperature profiles

The 0000 UTC composite sounding profiles for the NT, WT, and ST cases are displayed in Fig. 8. The surface temperature (dewpoint) for the NT composite

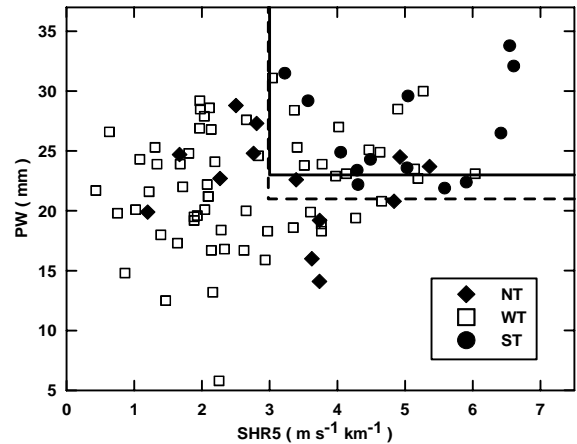


Fig. 7. Scatter plot of PW versus SHR5 for the 87 Alberta storms categorized into NT (diamonds), WT (squares) and ST (dots) cases. The solid (dashed) line marks the 77% (100%) threshold for ST events.

(Fig. 8a) was about 22 (13) $^{\circ}\text{C}$ and 20 (12) $^{\circ}\text{C}$ for the WT composite (Fig. 8b). The ST composite (Fig. 8c) had a surface temperature of about 22 $^{\circ}\text{C}$ and the greatest dewpoint of 14 $^{\circ}\text{C}$. The most unstable LCL (MULCL) for all cases were similar at about 1 km AGL. The MUCAPE was greatest for the NT composite at 1250 J kg^{-1} , lowest for the WT at 540 J kg^{-1} and about in the middle of the other two for the ST composite with a value of 850 J kg^{-1} . Higher values of MUCAPE were not associated with the tornado composites suggesting, again, there is little relationship between CAPE magnitude alone and the potential for thunderstorms to be tornadic. The Lifted Index for the NT, WT, and ST composites are -5 , -3 and -4 respectively, indicating convection is possible.

5.2 Hodographs

Composite hodographs for NT, WT and ST cases are shown in Fig. 9. The hodographs for the WT and ST composites (Figs. 9b and 9c respectively) show veering winds in the low levels (below $\sim 800 - 750 \text{ mb}$) similar to the results for supercell storms in Alberta. Chisholm and Renick (1972; hereafter referred to as C&R). Meanwhile the NT composite (Fig. 9a) had very light winds near the surface becoming almost unidirectional from the southwest above 850 mb . The ST composite hodograph (Fig. 9c) showed the most striking resemblance to the supercell hodograph of C&R with strong veering of the winds below $\sim 750 \text{ mb}$. Winds veered from east at $\sim 2 \text{ m s}^{-1}$ at the surface to southwest $\sim 8 \text{ m s}^{-1}$ at 750 mb . The wind at 500 mb (southwest $\sim 16 \text{ m s}^{-1}$) and at 300 mb (southwest $\sim 28 \text{ m s}^{-1}$) was similar to findings of C&R for supercells. The hodograph for the NT composite (Fig. 9a) showed light winds near the surface with weak veering below 800 mb and overall lower speeds than the ST case. Wind speeds increased throughout the sounding to southwest 20 m s^{-1} at 300 mb .

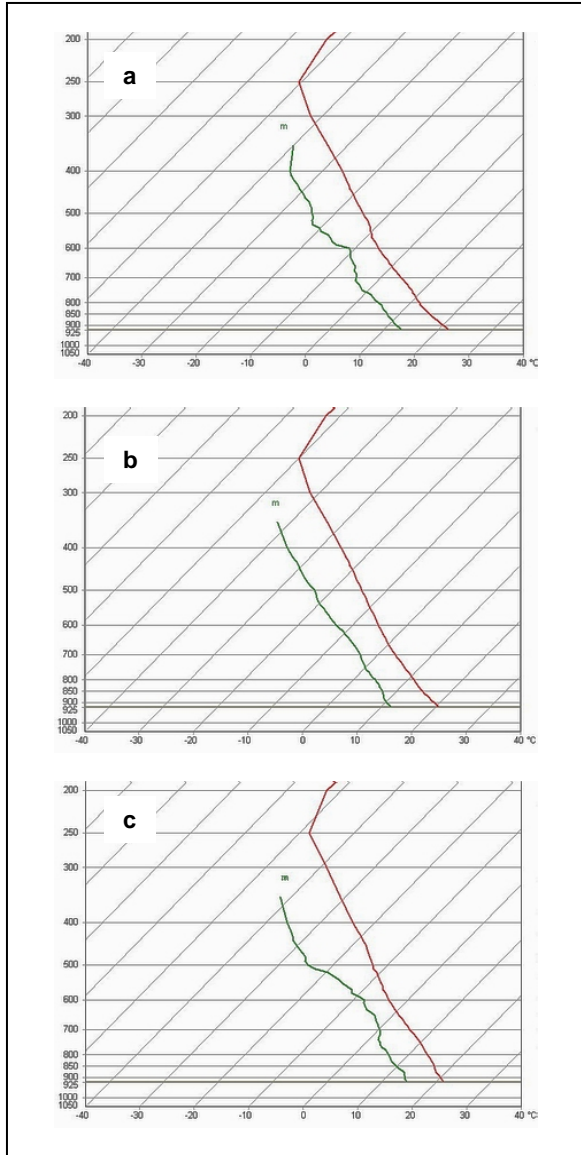


Fig. 8. Skew T-log p diagrams at 0000 UTC for the composite soundings of a) NT events, b) WT events, and c) ST events. The plot on the right is the temperature ($^{\circ}\text{C}$) and the plot on the left is the dewpoint ($^{\circ}\text{C}$).

According to C&R, the NT hodograph would be indicative of multicell rather than supercell storms. The WT hodograph (Fig. 9b) had the lowest overall wind speeds. There was weaker veering below 800 mb compared to the ST hodograph. Surface winds were southeast 1 m s^{-1} and veered to south-southwest 3 m s^{-1} at 750 mb. Winds at 300 mb were southwest 13 m s^{-1} .

6. SUMMARY AND DISCUSSION

We investigated the usefulness of selected sounding parameters for discriminating between significant

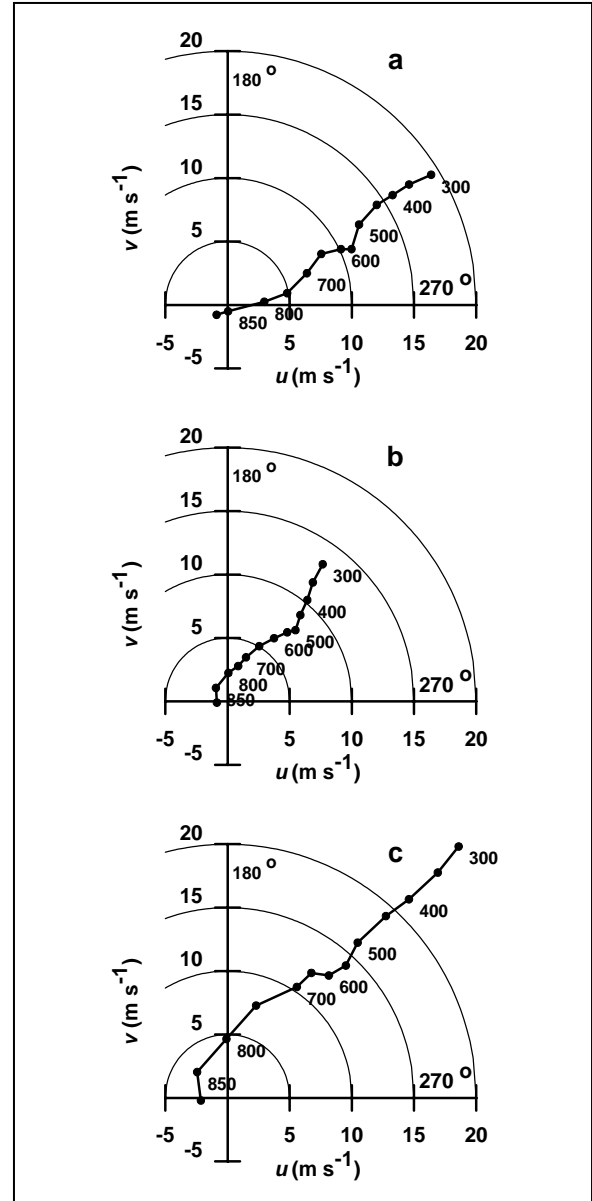


Fig. 9. Hodograph diagrams at 0000 UTC for a) NT , b) WT , and c) ST composites. Wind speeds are in m s^{-1} . Values (black dots) are plotted at 50 mb intervals from 900-300 mb. Numbers along the plot are pressure levels in mb.

tornado (ST), weak tornado (WT) and non-tornadic severe thunderstorm (NT) events. This study is built on the premise that the formation of a tornado is conditional on the prior formation of a severe thunderstorm and is not intended as a means to predict development of thunderstorms. Sounding parameters related to the wind regime, such as bulk shear from 900-500 mb, low-level shear from 900-800 mb, and 0-3 km storm-relative helicity provided help to distinguish ST events from both NT and WT events. Bulk shear within the 900-500 mb

layer (SHR5) showed statistically significant differences for values between the NT, WT and ST events. Threshold pairs of deep layer and low-level shear (SHR5, SHR8) may provide probabilistic guidance for determining the conditional potential for significant tornadoes. For example threshold pairs of (SHR5 = 3 m s⁻¹ km⁻¹, SHR8 = 6 m s⁻¹ km⁻¹) would have captured roughly about 75% of the ST cases. Precipitable water provided discrimination of ST events from both NT and WT events. Similar to the shear threshold pairs the data suggest that threshold pairs of deep layer shear and PW may also provide probabilistic guidance for determining the conditional potential for significant tornadoes. Threshold pairs of SHR5 = 3 m s⁻¹ km⁻¹ and PW = 23 mm would have captured roughly 75% of the ST cases.

Composite soundings showed the highest value of MUCAPE (1250 J kg⁻¹) was associated with the NT case. Higher values of MUCAPE were not associated with the tornado composites. Calculations of buoyancy related parameters such as CAPE and stability indices should be used with caution since they are sensitive to low-level moisture. The hodograph for the ST composite was similar to that found for the supercell storms in Alberta with strong veering of the winds from east in the low-levels to southwest in mid-levels. The WT hodograph showed less veering and lower speeds than the ST hodograph, while the NT hodograph had almost unidirectional winds. These results may suggest the ST events were likely spawned from supercells while some of the NT and WT events might have been associated with non-supercell storms

The shortcomings and complications inherent to our empirical study are discussed in Dupilka and Reuter (2006b). A major issue is to what extent the observed sounding data released from WSE at 0000 UTC are indeed representative for the airmass which feeds the severe storms. Our study also is also limited by the relatively small number of significant tornado events. These cases are rare and are coupled with the sparseness of upper air stations in Alberta. The problem of sounding scarcity in Alberta is not likely to change in the foreseeable future.

Our results on shear and precipitable water threshold values should be considered in a probabilistic manner. That is, within the parameter space there are regions where, given the development of a thunderstorm, the probability of that thunderstorm becoming tornadic is greater than in other areas. Additionally, there are regions in the parameter space where a given thunderstorm has a greater potential to develop a significant tornado.

7. REFERENCES

Bluestein, H. B., and M. H. Jain, 1985: Formation of mesoscale lines of precipitation: Severe squall lines in Oklahoma during the spring. *J. Atmos. Sci.*, **42**, 1711-1732.

- Brooks, H. E., C. A. Doswell III, and J. Cooper, 1994: On the environment of tornadic and non-tornadic mesocyclones. *Wea. Forecasting*, **9**, 606-618.
- Bunkers, M. J., B. A. Klimowski, J. W. Zeitler, R. L. Thompson, and M. L. Weisman, 2000: Predicting supercell motion using a new hodograph technique. *Wea. Forecasting*, **15**, 61-79.
- Chisholm, A. J., and J. H. Renick, 1972: The kinematics of multicell and supercell Alberta hailstorms. Research Council of Alberta Hail Studies Report 72-2, 7 pp.
- Davies-Jones, R. P., D. Burgess, and M. Foster, 1990: Test of helicity as a tornado forecast parameter. Preprints, *16th Conf. on Severe Local Storms*, Kananaskis Park, AB, Canada, Amer. Meteor. Soc., 588-592.
- Doswell, C. A., III, and E. N. Rasmussen, 1994: The effect of neglecting the virtual temperature correction on CAPE calculations. *Wea. Forecasting*, **9**, 625-629.
- Dupilka, M. L., and G. W. Reuter, 2006a: Forecasting tornadic thunderstorm potential in Alberta using environmental sounding data. Part I: Wind shear and buoyancy, *Wea. Forecasting*, **21**, 325-335.
- _____, and _____, 2006b: Forecasting tornadic thunderstorm potential in Alberta using environmental sounding data. Part II: Helicity, precipitable water, and storm convergence. *Wea. Forecasting*, **21**, 336-346.
- Hage, K. D., 2003: On destructive Canadian prairie windstorms and severe winters. *Natural Hazards*, **29**, 207-228.
- Klemp, J. B., 1987: Dynamics of tornadic thunderstorms, *Annu. Rev. Fluid Mech.*, **19**, 369-402.
- Markowski, P. M., J. M. Straka, E. N. Rasmussen, and D. O. Blanchard, 1998: Variability of storm-relative helicity during VORTEX, *Mon. Wea. Rev.*, **126**, 2959-2971.
- _____, _____, and E. N. Rasmussen, 2002: Direct surface thermodynamic observations within the rear-flank downdrafts of nontornadic and tornadic supercells. *Mon. Wea. Rev.*, **130**, 1692-1721.
- Miller, I., J. E. Freund, and R. A. Johnson, 2000: *Probability and Statistics for Engineers*. 4th ed. Prentice Hall, 612 pp.
- Rasmussen, E. N., and R. B. Wilhelmson, 1983: Relationships between storm characteristics and 1200 GMT hodographs, low level shear and stability. Preprints, *13th Conf. on Severe Local Storms*, Tulsa, OK, Amer. Meteor. Soc., 55-58.
- _____, and D. O. Blanchard, 1998: A baseline climatology of sounding-derived supercell and tornado forecast parameters. *Wea. Forecasting*, **13**, 1148-1164.
- Thompson, R. L., R. Edwards, J. A. Hart, K. L. Elmore, and P. Markowski, 2003: Close proximity soundings within supercell environments obtained from the Rapid Update Cycle. *Wea. Forecasting*, **18**, 1243-1261.